A new evidence base to document millennial changes in coastal vegetation

Nicole Foster

nicolefoster007@gmail.com

University of Adelaide https://orcid.org/0000-0001-7159-7391

Alice Jones

https://orcid.org/0000-0002-6157-2024

Oscar Serrano

Centre for Advanced Studies of Blanes, (CEAB-CSIC)

Anna Lafratta

Edith Cowan University

Paul Lavery

Edith Cowan University

Kor-jent Van Dijk

The Universtiy of Adelaide

Ed Biffin

Botanic Gardens and State Herbarium of South Australia

Bronwyn Gillanders

The University of Adelaide

Jennifer Young

Flinders University

Pere Masque

Edith Cowan University https://orcid.org/0000-0002-1789-320X

Patricia Gadd

Australian Nuclear Science and Technology Organisation

Geraldine Jacobsen

Australian Nuclear Science and Technology Organisation https://orcid.org/0000-0002-9644-5877

Atun Zawadzki

Australian Nuclear Science and Technology Organisation

Andria Greene

California State University

Michelle Waycott

University of Adelaide

Article

Keywords:

Posted Date: October 12th, 2023

DOI: https://doi.org/10.21203/rs.3.rs-3378191/v1

Additional Declarations: There is **NO** Competing Interest.

Version of Record: A version of this preprint was published at Communications Earth & Environment on March 6th, 2024. See the published version at https://doi.org/10.1038/s43247-024-01277-y.

Abstract

Anthropogenic activities are causing detrimental changes to coastal plants– namely seagrass, mangrove, and tidal marsh. Looking beyond recent times and to past vegetation dynamics is critical to assess the response and resilience of an environment to change. Here, we develop a novel multi-proxy approach, providing a new evidence base to decipher long-term change in coastal plant communities. Combining targeted environmental DNA analysis with chemical analysis of soils, we reconstructed 4,000 years of change at a temperate wetland and identified an ecosystem shift that occurred between ~ 1000 and 2000 years ago. What was a previous subtidal seagrass system shifted to an intertidal mangrove environment at present. We demonstrate that high-resolution information on millennial changes in coastal vegetation can be attained through these proxies. This approach could be applied to other ecosystems to improve the way we protect, conserve, and restore vegetated ecosystems.

Introduction

Life within the ocean relies on coastal marine plants such as seagrasses, mangroves and tidal marshes to provide habitat, protection and nurseries for a multitude of marine organisms[1]. These plant environments are vitally important to modern society for their ability to store carbon, stabilise coastlines and support food webs, yet they are under decline from anthropogenic change[2]. The era of Industrial Revolution urbanisation became a turning point for rapid degradation in coastal environments, but these habitats have experienced a history of change over geologic timescales (e.g., sea level rise and fall, climate, mass extinction, and plate tectonics). Uncovering historical change and identifying tipping points in ecosystem conditions are necessary for contextualising present day changes, understanding natural resilience and successfully restoring degraded coastal habitats[3].

Successful restoration relies on what we deem as the natural state of the system. This natural state is arbitrary and is often impacted by the shifting baseline syndrome – what we perceive as the natural state is only what has been measured in our lifetime[4]. This skewed perspective means restoration goals can often be unattainable or set up to fail. Incorrectly perceiving the natural state of an environment usually stems from a lack of data over meaningful timescales[5]. Traditional methods for assessing historical change in coastal plants include archival observations, which can be biased and only provide information at the scale of decades[6]. Information on deeper time scales comes from the analysis of multiple proxies, like isotopes, fossils (in the form of plant fragment remains) and pollen trapped in natural archives[7]. For example, soil core archives can be dated, and historical reconstructions inferred. However, the fossil record is skewed toward plants that deposit material readily and relies on expertise to identify the remains[8]. This can be time consuming and lead to low taxonomic resolution or inaccurate estimates of community composition, prompting a need for more accurate methods to assess change over time in coastal vegetated environments.

The recovery and analysis of environmental DNA (eDNA) from soil cores is a promising tool for historical reconstructions of coastal plant communities[9–11]. When these data are coupled with information on the environmental conditions of a site, a detailed picture of environmental change can emerge[12]. Here, we analysed four soil cores, applying multiple proxies to look at environmental change in a temperate wetland (Fig. 1). This wetland is presently dominated by mangrove (*Avicennia marina*) and cores were specifically taken here due to the high sedimentation rates and the dense root systems of mangroves that work to stabilise the sediment[13]. This stabilisation ensures a coherent stratigraphy, justifying their use as soil archives that can be dated. We documented 4000 years of historical change at this site and implemented targeted capture of eDNA over the traditional metabarcoding approach to capture multiple chloroplast gene regions and improve the ability to detect coastal plants. We combined this with the analysis of chemical proxies to build multiple lines of evidence for past changes. This proof-of-concept study successfully reconstructed millennial ecosystem changes in a temperate wetland, demonstrating the potential for implementing these analyses in other environments to better understand and manage plant communities into the future.

Results

All four soil cores analysed in this study corroborate that this study site was historically a subtidal seagrass system that shifted to an intertidal mangrove habitat. This change was defined by increasing downcore trends in the following variables; subtidal vegetation (detected with eDNA), $\delta^{13}C$, dry bulk density, Calcium/Iron (Ca/Fe) and Strontium (Sr) (normalised to Molybdenum incoherent + coherent scattering), and decreasing downcore trends in the following variables; intertidal vegetation, $\%C_{org}$, Molybdenum Compton (incoherent) and Rayleigh (coherent) scattering (Moly ratio), Titanium/Calcium (Ti/Ca) and Bromine/Chlorine (Br/Cl). These trends were used to define two stratigraphic units in the soil profile, the separation of which occurred ~ 1000–2000 years ago based on radiocarbon dating and detection of a hiatus (jump in ages) around this period (Fig. 2A, Table S3). This hiatus prevented the construction of age-depth models and so change point analyses were performed on the decompressed depths. Significant change points were detected at 63 cm for $\%C_{org}$, $\delta^{13}C$ and dry bulk density, and at 60 cm for Moly ratio, Ti/Ca, Br/Cl, Sr, Ca/Fe (with a confidence value of 1 – maximum confidence). This defined the two units in the soil profile; Unit 1 ~ 0–60 cm (< 1000 years BP) and Unit 2 ~ 60–100 cm (> 2000 years BP). These two Units represent distinct ecosystems from a subtidal seagrass envrionment ~ 4000 years ago in Unit 2 to an intertidal mangrove system in Unit 1, illustrating an ecosystem shift has occurred at this site.

Environmental DNA

Plant communities detected using eDNA for all soil cores indicate intertidal and high intertidal plants were present in both Unit 1 and 2 but as intertidal plants decreased in relative abundance in Unit 2, subtidal plants increased. Subtidal vegetation increased exponentially over time (edf = 2.3, $P < 0.05$) but intertidal vegetation decreased linearly (edf = 1.0, $P < 0.05$) and high intertidal vegetation did not change

(edf = 1.988, P = 0.3; Fig. 2B), which was justified across all four soil cores (non-significant (P = 1) random effect of core) and illustrates changing community structure over time. The community structure in Unit 2 comprised subtidal plants, particularly the seagrass *Zostera nigricaulis*, which was only observed once in Core 1 but multiple times in Cores 2, 3, and 4 with maximum relative abundances of 32%, 40%, 66% and 32% respectively. Additional subtidal plants detected in Unit 2 (all < 10% of the total community) were *Posidonia australis* and *Ruppia maritima* in Cores 2 and 4, and *Amphibolis antarctica* in Core 2, Fig. 2C. The plant community in Unit 1 was dominated by the intertidal mangrove species *Avicennia marina*, comprising 100% of the community in some instances, Fig. 2C. Additional detections of intertidal species were only made at a single depth in Core 1 which were of the family *Chenopodiaceae.* High intertidal plant communities were detected throughout all four soil cores but never exceeded 35% of the total community. These high intertidal plants consisted of *Myoporum insulare* (Scrophulariaceae) and Convolvulaceae (*Wilsonia humilis*) with additional plant species detected at a single depth in Core 1, Aizoaceae (*Disphyma crassifolium*) and Primulaceae (*Samolus repens*), Fig. 2C.

$\%C_{org}$, $\delta^{13}C$, dry bulk density

The measured variables $\delta^{13}C$ and dry bulk density (DBD) were higher in Unit 1 and $\%C_{org}$ was lower (Figure S3), presenting evidence for a shift in environmental conditions between Units 1 and 2 (Fig. 3A). This was illustrated with a Principal Component Analysis where principal component 1 explained 73.9% of the variance. All variables contributed similarly to principal component 1 (PC1) with $\delta^{13}C$ contributing the greatest to the observed change (37%) followed closely by DBD (33%) and $\%C_{org}$ (30%) (Table S2). All measured variables were strongly correlated with PC1 ($R^2 > 0.6$), supporting the use of this principal component for identifying significant change points, with one identified at 63 cm, defining the shift in environmental conditions.

X-ray Fluorescence

Chemical elements measured using X-ray Fluorescence (XRF) confirmed changing environmental conditions from Unit 1 to 2 (Fig. 3B). Ca/Fe and Sr increased over time and the Moly ratio, Ti/Ca and Br/Cl all decreased over time (Figure S3). When these variables were analysed using principal components, principal component 1 (PC1) explained 76.4% of the variance. Sr contributed the most to this variation (24%, Table S2) followed by Br/Cl, Moly ratio, Ca/Fe and Ti/Ca was the lowest contributor (13%). All variables strongly correlated with PC1 ($R^2 > 0.7$) except Ti/Ca which was only moderately correlated with PC1 ($R^2 = 0.5$). This justified using PC1 to identify significant change points, where one was identified at 60 cm, supporting a change in elemental composition of soils between Unit 1 and Unit 2.

Discussion

Long term change dynamics of coastal plant communities are important to understand their responses and resilience to changing environmental conditions[8]. In this study, we have demonstrated that coupling

targeted capture of eDNA with chemical analysis of soils provides high resolution reconstructions of coastal plant changes through time. We identified a historical ecosystem shift from a subtidal seagrass environment to the present-day intertidal mangrove habitat. This shift was characterised in all four soil profiles that we analysed and separated two stratigraphic Units; Unit 1, < 1000 years BP and Unit 2 > 2000 years BP. Using the combined approach of targeted eDNA and chemical analyses, we could build multiple lines of evidence for the 4000-year history of this temperate wetland (Fig. 4).

The present-day habitat (Unit 1) of our study site is a temperate wetland dominated by mangrove (*Avicennia marina*) which was captured in the eDNA results throughout all four cores. Given that environmental conditions indicate Unit 2 was a subtidal environment, mangrove detection is unlikely at that time. It is more likely this signal is an artefact of mangrove roots growing through the core as these can grow up to one meter[14]. While this works to maintain a clear chronology, it may not be reflective of the plant community at deeper timescales, especially given additional support that this was previously a subtidal community. eDNA signals confirmed the presence of multiple subtidal seagrass species in Unit 2; *Z. nigricaulis, R. maritima*, *P. australis* and *A. antarctica*, where the first two species can be found in shallow water and the latter two are typically found in deeper waters (> 1m)[15], indicating a higher sea-level was likely present in Unit 2. This is supported by evidence in [16] that this region had a higher sea level ~ 6000 years ago and it is hypothesised the sea level slowly dropped to present day conditions.

Indeed, the sea level at the site today supports intertidal communities with some high intertidal plants occurring in the adjacent landscape. This could explain the eDNA signals from high intertidal plant families detected throughout the four soil cores, where this is the result of detrital material being brought into the system, rather than these plants growing at the specific site the cores were taken. Plant material is known to be imported and exported within coastal landscapes and can end up sequestered in the soils of adjacent habitats[17]. We may have detected eDNA from adjacent habitats due the targeted eDNA approach designed for multiple chloroplast gene regions which increased our sensitivity beyond traditional single gene approaches[18,19]. These more traditional (metabarcoding) approaches rely on the amplification of target gene regions using primers. This can cause amplification bias as the corresponding primer binding sites may not be intact in degraded DNA from soil samples and primers can be biased towards amplifying specific taxa[20]. Targeted capture of eDNA does not rely on this initial amplification step and improves the likelihood of recovering all taxa present in a given sample because multiple genes are targeted[19,21,22]. This could make it difficult to know whether an eDNA signal is from a plant present at the study site or an adjacent one. Fortunately, pairing the eDNA results with environmental proxies identified conditions likely to support mangroves in Unit 1 and seagrasses in Unit 2.

Distinct environmental conditions were identified within Units 1 and 2, separating an intertidal environment from a subtidal one. This intertidal environment was characterised by high levels of organic matter as evidenced by the $\%C_{org}$ results and supported by higher values for the Moly ratio, which is an indication of organic matter content[23]. Higher organic matter in Unit 1 was also observed in the greater

Br/Cl values, signifying marine organic matter[24] and an increase in salinity downcore to Unit 2, which indicates a marine environment. Increased values of Sr in Unit 2 validate this[25], as well as a higher ratio of Ca/Fe – a proxy for carbonate productivity[26]. Seagrass presence in Unit 2 is further supported by higher values of $\delta^{13}C$, and while we could not use these values to reliably infer plant community presence (as $\delta^{13}C$ values can be influenced by mangrove roots[27] and organic matter diagenesis[28]) we can conclude this unit is more marine (seagrass) in nature than Unit 1 which has a more terrestrial influence. The terrestrial signal in Unit 1 stems from the higher Ti/Ca which is a proxy for terrigenous sediment supply[24,25]. However, within this Unit, we observed a spike in this ratio at ~ 25cm (Figure S3), explaining the low correlation to PC1. This proxy may be driven by a specific event or a changing sediment regime that occurred in Unit 1 at this time[16]. Regardless, the comparison of Ti/Ca between Unit 1 and Unit 2 supports Unit 1 as an intertidal environment. These characteristic environmental conditions for Units 1 and 2 validate that this site was a marine environment that supported a subtidal seagrass community that then shifted to a more terrestrial environment with higher organic content, supporting the present-day mangrove habitat.

The environmental conditions characterised by the four soil profiles builds a framework to interpret the eDNA results and by combining these proxies, a holistic picture of change has emerged. This picture describes a previous community of subtidal plants and a higher sea-level than present day that then shifted to an environment with a lower sea level where mangrove plants could thrive. There is evidence to suggest this shift occurred due to tectonic uplift [29], dramatically reducing sea level and paving the way for mangroves to colonise the area which would have exposed the soil surface to erosion and could explain the gap (hiatus) in the dating profile. This did not necessarily need to be a sudden event, as sea level could have dropped gradually to induce erosion, or this could have been caused by a major storm. The possible causes of the ecosystem shift are difficult to decipher but the synergies between targeted capture of eDNA, and chemical proxies of the soil, enabled this shift to be detected and a clear colonisation of mangroves into seagrass habitat was documented. These multiple lines of evidence for historical dynamics in coastal plants can be employed in other vegetated environments prone to change i.e., coastal sites at the interface of sea level rise, permafrost in locations of warming, to develop high resolution historical reconstructions. This will lead to an improved understanding of long-term change dynamics facilitating the protection, conservation, and restoration of vegetated ecosystems.

Materials and Methods

Study site

Four soil cores were collected from Torrens Island, South Australia (-34.7929, 138.5265). Historically, Torrens Island was occupied by the Kaurna people[30], the Traditional Owners of the land. The island is currently unoccupied and most of the site was declared a Conservation Park in 1972 to protect the diverse animal and plant life found there, including mangroves, temperate saltmarshes and seagrasses. Common species include *Atriplex paludosa, Wilsonia humilis, Disphyma crassifolium, Samolus repens,*

Suaeda australis, see [31] for a complete list); samphire shrublands dominated by *Sarcocornia, Salicornia* and *Tecticornia* species; and one mangrove species (*Avicennia marina*). The seagrass communities surrounding the island include *Posidonia* spp., *Zostera spp., Amphibolis* spp. and *Halophila* spp.[32]

Soil core collection and processing

Four soil cores (~ 1 m long and 7.5 cm wide) were collected in PVC pipes using manual percussion and rotation in 2017 (TI2.2017; Core 1) and 2018 (TIN1.2018, Core 2; TIN2.2018, Core 3; TIN3.2018, Core 4). Compression during coring was assessed by measuring the length of the corer protruding above the soil's surface both inside and outside the PVC pipe before retrieving the core. These measurements were used to calculate a compression rate that enabled back-calculation of decompressed sample depths after the core was sectioned[33]. Following retrieval, each core was sealed at both ends, transported vertically, and stored at 4°C until it was processed in the laboratory. Core 3 was sliced lengthways, with an intact half retained for scanning X-ray fluorescence (details below) and the remaining half treated as per the following description for all other cores. Throughout the soil sample preparation, steps were taken to reduce eDNA contamination, including wiping all laboratory benches with bleach, water and ethanol, and cleaning all equipment with ethanol between each sample[34].

The soil cores were sliced into 0.5 cm thick increments in the top 20 cm and at 1 cm thick increments for the remainder of each core. Each slice was weighed then a 0.5 g sub-sample was taken for DNA analyses and the remainder of the soil was dried at 60°C until constant dry weight to estimate dry bulk density (DBD). One sub-sample of the dried bulk soil was used for ^{14}C (age-dating) analysis. Another sub-sample was ground in a ball mill grinder and analysed for soil organic carbon content ($\%C_{org}$), with some of these sub-samples also being analysed for organic carbon stable isotopes ($\delta^{13}C$). A summary of the analyses done on each core is provided in Table 1 with further details on the sample preparation associated with each analysis described in the sections below.

Table 1. Summary table showing the sample analyses that were performed on the sediment samples from each core. Number of samples analysed for each variable are indicated in parentheses.

Core ID	eDNA	^{14}C dating	XRF	Dry bulk density	$\delta^{13}C$	%OC bulk
Core 1 (TI2.2017)	✔ (28)	✔ (5)	X	✔ (30)	✔ (30)	✔ (30)
Core 2 (TIN1.2018)	✔ (32)	✔ (4)	X	✔ (21)	✔ (21)	✔ (21)
Core 3 (TIN2.2018)	✔ (30)	✔ (2)	✔	✔ (19)	✔ (19)	✔ (19)
Core 4 (TIN3.2018)	✔ (30)	✔ (3)	X	✔ (19)	✔ (19)	✔ (19)

eDNA analysis

Extraction

A 0.5 g sub-sample of soil was collected from the middle of each soil slice and was stored at 4°C in Powerbead solution buffer (QIAGEN) until DNA extraction. Collecting from the middle of the slice helped prevent contamination (as the outside edges had been in contact with the PVC pipe). Each 0.5 g soil sample was divided into two equal weight (250 mg) replicates (A and B). DNA was extracted from each replicate sample using the DNeasy Powerlyzer Soil Kit (QIAGEN) with zirconia beads and using strict handling protocols to prevent contamination. We chose this extraction kit based on in-house trials and previous research[19,35] and used zirconia beads instead of the standard glass beads to ensure plant cells could be properly lyzed (personal observation). Post extraction is usually followed by sonication in targeted capture analyses[36], however, due to the degraded nature of DNA in soils[37] the impact of sonication on plant community recovery was tested before proceeding. A subset of samples from Core 1 were sonicated using a Diagenode Bioruptor® Pico to a size distribution peaking around 400–600 base pairs (bp) (cycle of 15 s on, 90 s off and repeat 7 times). Sonication reduced the number of unique taxa recovered in older sediment samples due to fragmenting already degraded DNA, whereas in recent samples sonication did not impact the number of unique taxa recovered (Figure S1). Based on this, all samples were processed without sonication, along with extraction blank controls to monitor contamination[34].

Library preparation

An aliquot of the DNA extract was placed into the NEBNext Ultra II Library preparation kit (New England Biolabs®) following manufacturer's instructions with the following modifications: 1/3 the recommended reaction volume (16.7 µL) and custom-made stubby (incomplete, P5 and P7 indexes missing) Y-adaptors (25uM)[38] were used at the ligation step. The design of these adapters replaced the uracil excision in the Ultra II protocol as instead, DNA underwent end repair then A-tailing, prior to ligating Y-adapters. Each adaptor had a unique 8 nucleotide barcode, giving each sample a unique pair of identical internal molecular identifiers (identified as the 8 first base calls for each read). Following adapter ligation, libraries were amplified to detectable concentrations using the supplied Q5 Master Mix at the original reaction volume of 50 µL with in-house primers P7 preCap Long and P5 preCap Long (Cycling conditions: [98°C 10 s, 65°C 30 s, 72°C 30 s] x 17 cycles, 72°C 120 s, 4°C hold). 2 µL of each uniquely indexed library was then visually checked using gel electrophoresis (1 x TE buffer, 1.5% agarose gel for 40 minutes at 80V) and pooled according to concentration estimates (determined via visual inspection) into batches of 8 samples and then purified using AMPure XP (at 0.8 x volume concentration) to remove remaining primers and other impurities.

Multi-gene region bait capture

We used the RefSeq release of plastid sequences (https://ftp.ncbi.nlm.nih.gov/refseq/release/plastid/: accessed Oct 2017) across ~ 160 taxa to design probes targeting a set of 20 plastid gene regions for angiosperms (Table S1) including standard plant barcoding regions[39]. Using *Arabidopsis lyrata* (Genbank reference NC_034379) as a reference, target regions were extracted from the RefSeq data using Blast (blastn, e value < 1e-50) and were clustered using CD-HIT[40] with a 95% identity cut-off, retaining the

longest sequence per cluster for probe design. A total of c. 2800 representative sequences, ranging in length from 180–900 bp (mean 370 bp) were used to design c. 15,000 120-mer probe sequences with 2X tiling (i.e., each probe overlaps half its length). Further information can be found in [41].

Targeted capture was performed on each batch of libraries following the myBaits® Targeted NGS Manual Version 4.01 as per the manufacturer's instructions. The hybridisation temperature/time was 65°C for 48 hours. Following hybridization, the product was amplified using custom P7 and P5 indexed primers designed in-house using cycling conditions: 98°C 120 s, [98°C 20 s, 60°C 30 s, 72°C 45 s] x 17 cycles, 72°C 30 s, 4°C hold. The final product was an Illumina library where each sample had a unique combination of identical internal dual barcodes (incorporated during library preparation) and two indexes (incorporated after hybridisation). Within our laboratory, all dual barcode-Index 1-Index 2 combinations are only used once, thus reducing contamination risk.

Following targeted capture and amplification, the resulting libraries were run on a 2100 Bioanalyzer (Agilent) using the high sensitivity DNA assay and molarity was calculated between 300–800 bp. All libraries were then pooled in equimolar concentration and purified using AMPure XP (New England Biolabs) at 0.7 x concentration to remove primer dimer and short sequences. The final library underwent further size selection using a Pippin Prep (Sage Science) with a 1.5% agarose gel cassette set to select between 300–600 bp. The resulting library was quantified using a QuantStudio 6 Flex Real-Time PCR (Thermo Fisher Scientific) and sent to the Garvan Institute of Medical Research (Sydney, Australia) to be sequenced on one lane of an Illumina HiSeq X Ten using 2x150 bp chemistry. Full details of library preparation and targeted capture can be found in[41].

Bioinformatics

Full details for bioinformatic processing of sequences can be found in [19] and all scripts including the reference sequence database used in this study are available on Github (https://github.com/NicoleRFoster/Targeted-capture-of-eDNA-in-sediment-cores).

For read processing and mapping, raw sequences were demultiplexed based on indexes using Illumina Bcl2fastq v2.18.0. The output Read 1 and Read 2 fastq.gz files were then demultiplexed based on the Y-adapter internal barcodes using AdapterRemoval v2[42]. PALEOMIX[43] was used to trim adapters (using AdapterRemoval), discard sequences less than 25 bp and trim for ambiguous nucleotides and low-quality base calls. BWA-MEM aligner[44] was selected within PALEOMIX as the mapping tool with a mapping quality of 30 and discarding unmapped reads. A specified reference database was made by combining the temperate coastal plant reference database from [45] with a curated database from the National Centre for Biotechnology Information[46] that contained all plants (both terrestrial and coastal) within the local sampling location. Following mapping, Picard Mark Duplicates (Version 4.0.10.1) was used to remove clonality (duplication in read alignment) and the resulting BAM files were then used to generate VCF files using SAMtools mpileup[47], specifying ploidy as 1 (as haplotypic organellar DNA) and filtering for base quality < 30, mapping quality < 30 and depth < 50, outputting N's if read coverage was not met. Variant

calls were normalised with BCFtools norm[47] and the consensus caller in BCFtools was then used to call final consensus FASTA files, outputting variants with N's.

Despite stringent mapping, some of the gene regions may be unable to distinguish among closely related species and/or the correct species in the sample is not represented in our database. For example, a specific gene region may only be capable of separating taxa at the family level and therefore reads may not map to this region for the specific species in the sample, instead mapping to this region for a species not in the sample but from the same family. To overcome this issue, we clustered that data by assigning rankings to consensus FASTA sequences based on the ability of the sequence to distinguish taxa at the Order, Family, Genus or species level. To do this, FASTA files were filtered for length < 100 bp and all ambiguity and missing data codes were removed prior to clustering the reads with the reference database using CD-HIT-EST[40]. The threshold for sequence identity was set to 95%, length and clustering of sequences were specified to cluster at the most similar cluster and alignment was set to cover at least 10% of the representative sequence and 100% of the shorter sequence (-aL 0.1 -aS 1). If the sample consensus sequence clustered broadly with other sequences, it meant either, the gene in question did not have high enough variation to resolve taxonomy below a certain level, or the sample consensus sequence contained a high number of ambiguous base calls that confounded species identification i.e., read depth did not meet the assigned threshold to call a base (depth < 50 bp) and instead missing data values were inserted (N's).

For data processing, a custom script was written in R version 3.5.1[48] to unpack the output.clstr file from CD-HIT-EST and generate upstream taxonomic assignment for each sample, in each cluster. The script identified the highest common taxonomic ranking as an output for each cluster, denoting this as 'rank'. The final dataset contained assigned sample taxonomy generated from the mapping of reads and a ranking for the level of taxonomic clustering this sequence provided. This script was written using the R packages taxize[49], TAI[50], dplyr[51], stringi[52], stringr[53] and tidyr[54].

Replicate samples, A and B, were then combined to assess overall gene recovery for each section of the soil cores. Taxa with less than four gene regions recovered were not included in the final community evaluation (informed by recommendations in [19]). All samples were then combined for each core such that there was a single file documenting species recovery and taxonomic ranking for all samples analysed along the length of each core. These were then converted into separate phyloseq[55] objects and data were subset to only include taxonomic rankings at the family level or below (for visualisation purposes – species and genus level assignments were included in the interpretation of results). Taxonomic assignments were then summarised by families to calculate relative abundances as a percentage of total community composition at each position along each core.

To summarise changes in coastal plant communities through time, we designated three community types to the detected plant families. These were: subtidal (seagrasses), intertidal (mangrove and samphire) and high intertidal (other coastal plants). To assess changes in relative abundances of communities with depth across all four cores we fitted a generalised additive model using the gam function in the mgcv

package[56] in R[48]. We tested several models and used the lowest AIC and most variance explained by the model to select a final model candidate. This model included relative abundance as the response variable with community type as an explanatory variable, a smoothing term of depth by community type and including sediment core as a random factor.

Relative abundance ~ community type + s(depth, by = community type) + s(core, bs = "re")

The degree of smoothing was estimated using restricted maximum likelihood (REML).

Chemical analyses

Radiocarbon dating

Radiocarbon (^{14}C) analyses were conducted on three to five bulk soil sub-samples taken from below 22 cm in each core. The sampling depths from each core were selected based on taking one sample from just below the top section of the core (that was thought to be mixed based on previous studies); one sample from near the bottom of the core (the oldest soil); and at least one (and up to three) samples from in between these upper and lower sample positions. Radiocarbon dating was performed on bulk soil samples from Core 1 at the AMS Direct Laboratory (USA), and for the remaining three cores, at the Centre for Accelerator Science, Australian Nuclear Science and Technology Organisation (ANSTO). Carbonates and humic acids were removed by treating the sample with 2M HCl (at 60^{o}C) for carbonate removal, a series of sodium hydroxide (NaOH) treatments (at 60^{o}C) for the removal of humics and a final treatment of 2M HCl (at room temperature). After drying, the samples were combusted to carbon dioxide (CO_2) and reduced to graphite using H_2/Fe at 600^{o}C. The graphite targets were analysed by accelerator mass spectrometry (AMS) using the Vega 1MV NEC accelerator.

Radiocarbon ages were calibrated in OxCal 4.4.4[57] using a P-Sequence deposition model. Calibrations were performed against the SHCal20 calibration curve[58] or a mixed SHCal20/Marine20[59] curve where a marine influence is identified. Marine influence was corrected using a local ΔR = -150 ± 59 taken from the Australian ΔR calculator for the Torrens Island region (https://delta-r-calc.jcu.io/)[60].

The degree of marine influence was assessed based on the organic $\delta^{13}C$ stable isotope ratio (‰). Some of our samples had higher $\delta^{13}C$ values than would be expected in a 100% marine environment, indicating a mixed terrestrial/marine carbon source (as expected in estuarine settings, such as Torrens Island). For these samples we calibrated the dates using mixed curves, based on a value of -25.0‰ being 100% terrestrial, and a value of -10.0‰ being 100% marine. These thresholds assume that the marine organic inputs at our site would be primarily seagrass, and seagrass $\delta^{13}C$ stable isotope values typically range from − 13.3‰ to -7.3‰.

Dry bulk density, organic carbon and stable isotope analyses

Dry bulk density (DBD; g cm^{-3}) was calculated for all depth increments from all four cores (See Table 1 for number of analyses) using the dry weight data and sample volume. All samples were analysed for organic carbon (%) and stable isotope composition ($\delta^{13}C$).

For organic carbon (%), each dried bulk sediment sample was acid treated to remove inorganic carbon by adding 4% HCl. The sample was then centrifuged at 3,400 rpm for 5 min and the supernatant (including acid residues) was carefully removed with a pipette, avoiding resuspension. The pelleted soil sample was then washed with ultrapure water, centrifuged again, and the supernatant carefully removed. Post acid treatment, the remaining soil sample was re-dried at 60°C until a constant weight was achieved and then placed into a tin capsule for analysis. The % organic carbon was determined on the acid-treated samples using a Costech Elemental Analyzer at the University of Hawaii Hilo Analytical Laboratory, USA (Core 1 samples) or a Perkin Elmer EA2400 Series II at the MASS Facility, in the SET Faculty at the University of Adelaide, Australia (samples from Cores 2–4), with calibration against an Acetanilide certified reference standard.

The acid pre-treated dried bulk soil samples were also used for organic carbon stable isotope analyses ($\delta^{13}C$). A mass of sample equivalent to 100 µg of organic carbon was accurately weighed into a tin capsule based on the organic carbon content determined by the elemental analyses (as described above). The weighed samples from Cores 2–4 were analysed for $\delta^{13}C$ using a continuous flow isotope ratio mass spectrometer (Nu Horizon, Wrexham, UK) equipped with an elemental analyser (EA3000, EuroVector, Pavia, Italy) at the MASS Facility, in the SET Faculty at the University of Adelaide, Australia, whereas samples from Core 1 were analysed using a Thermo-Finnegan Delta V Isotope Ratio Mass Spectrometer at the University of Hawaii Hilo Analytical Laboratory, USA.

For all samples, the stable isotope ratios were expressed in δ notation as deviations from a standard in parts per mil (‰):

$$\delta^{13}C = [(R_{sample}/R_{standard})\text{-}1] \times 1000.$$

Where R_{sample} is the ratio of abundance of ^{13}C /^{12}C in the sample, and $R_{standard}$ is this ratio in the standard. $\delta^{13}C$ was reported relative to the standard Vienna Pee Dee Belemnite (VPDB). All samples were corrected for instrument drift and normalized according to reference values using in-house standards (n = 19 per 60 samples); $\delta^{13}C$ = glycine − 31.2‰, glutamic acid − 16.7‰ & triphenylamine (TPA) -29.2‰ calibrated against USGS and IAEA certified reference materials (USGS40, USGS 41, IAEA-2, NIST 8704).

X-ray fluorescence (XRF)

A full length ½ longwise section of Core 3 was analysed using an Itrax XRF core scanner at the Australian Nuclear Science and Technology Organisation (ANSTO). This is a non-destructive method for rapidly generating high-resolution elemental profiles using XRF spectrometry. The Itrax XRF scans were performed using a molybdenum tube set at 55 kV and 30 mA with a dwell time of 10 s. A step size of 200

µm was selected to capture elemental variations occurring in laminations observed in the radiographic image. The Itrax XRF analysis produced data for a standard suite of 36 elements and Molybdenum Compton (incoherent) and Rayleigh (coherent) scattering. From these, we selected five elements/ elemental ratios that were most relevant to our research question, these were Moly ratio, Ti/Ca, Br/Cl, Sr and Ca/Fe where Sr was normalised against Molybdenum incoherent + coherent scattering to reduce the impact of water content and density changes in the soil core[61].

Data analysis

Assessing change in DBD, $\%C_{org}$, $\delta^{13}C$ and XRF

To reduce dimensionality and assess consistent downcore trends across DBD, $\%C_{org}$, and $\delta^{13}C$, we applied Principal Component Analysis (PCA)[62] to all four Cores. PCA analysis was run in R using the 'stats' package[48] and the function 'princomp' with data centred and scaled. We similarly applied a PCA to the five-element dataset produced by the XRF analysis on Core 3, to generate a single data point for each depth increment that represents the variance in all five elements/element ratios; Moly ratio, Ti/Ca, Br/Cl, Sr, Ca/Fe.

We subsequently used the outputs from both the PCA analyses (component 1 values for each depth increment) in a changepoint analysis, run in R using the package 'changepoint'[63] and the function 'cpt.meanvar'. Changepoint analyses statistically assess whether any significant, sustained changes in the mean and variance of a combined dataset have occurred (not assuming constant variance). The test identifies the number of changes and their position in the data series, and provides confidence estimates (0–1, with 1 being full confidence) for any changes detected. This approach allowed us to test for any clear inflection or change points in soil biogeochemistry through the core depth profiles.

All plots and figures presented in the results were created in R using the package ggplot[64]. The conceptual model of the system, which is based on the suite of data produced by our multiple analyses, was generated using the software Adobe Illustrator.

Declarations

Acknowledgements

Access to ANSTO facilities (Centre for Accelerator Science, ITRAX XRF and ^{14}C dating) was provided under ANSTO Award AP11907. We acknowledge the financial support from the Australian Government for the Centre for Accelerator Science at ANSTO through the National Collaborative Research Infrastructure Strategy (NCRIS). This work was supported by the Goyder Institute for Water Research (project reference: CA-16-04), with co-funding received from SA Water, the SA-EPA, ECU and the University of Adelaide's Environment Institute., a Herman Slade Foundation grant (HSF 18 – 2) awarded to AJ. A Max Day Environmental Fellowship awarded by the Australian Academy of Science to NF and a Research

Training Program Scholarship awarded to NF. OS was supported by I + D + i projects RYC2019-027073-I and PIE HOLOCENO 20213AT014 funded by MCIN/AEI/10.13039/501100011033 and FEDER. The IAEA is grateful for the support provided to its Environment Laboratories by the Government of the Principality of Monaco. Collection of soil samples was conducted under the State Herbarium of South Australia permit G25787-3. We would like to thank Luis Williamson for his assistance in the field.

References

1. Barbier, E. B. *et al.* The value of estuarine and coastal ecosystem services. *Ecol. Monogr.* **81**, 169–193 (2011).
2. Halpern, B. S. *et al.* Recent pace of change in human impact on the world's ocean. *Sci. Rep.* **9**, 11609 (2019).
3. Bálint, M. *et al.* Environmental DNA Time Series in Ecology. *Trends Ecol. Evol.* **33**, 945–957 (2018).
4. Pauly, D. Anecdotes and the shifting baseline syndrome of fisheries. *Trends Ecol. Evol.* **10**, 430 (1995).
5. McClenachan, L., Ferretti, F. & Baum, J. K. From archives to conservation: why historical data are needed to set baselines for marine animals and ecosystems. *Conserv. Lett.* **5**, 349–359 (2012).
6. Alleway, H. K. *et al.* The shifting baseline syndrome as a connective concept for more informed and just responses to global environmental change. *People Nat* **5**, 885–896 (2023).
7. Powell, T. M. & Steele, J. H. *Ecological Time Series*. (Springer Science & Business Media, 2012).
8. Foster, N. R., Gillanders, B. M., Jones, A. R., Young, J. M. & Waycott, M. A muddy time capsule: using sediment environmental DNA for the long-term monitoring of coastal vegetated ecosystems. *Mar. Freshwater Res.* **71**, 869 (2020).
9. Nguyen, N.-L. *et al.* Sedimentary ancient DNA: a new paleogenomic tool for reconstructing the history of marine ecosystems. *Front. Mar. Sci.* **10**, (2023).
10. Pedersen, M. W. *et al.* A comparative study of ancient environmental DNA to pollen and macrofossils from lake sediments reveals taxonomic overlap and additional plant taxa. *Quat. Sci. Rev.* **75**, 161–168 (2013).
11. Parducci, L. *et al.* Shotgun Environmental DNA, Pollen, and Macrofossil Analysis of Lateglacial Lake Sediments From Southern Sweden. *Front. Ecol. and Evol.* **7**, (2019).
12. Barrenechea Angeles, I. *et al.* Encapsulated in sediments: eDNA deciphers the ecosystem history of one of the most polluted European marine sites. *Environ. Int.* **172**, 107738 (2023).
13. Pérez, A., Libardoni, B. G. & Sanders, C. J. Factors influencing organic carbon accumulation in mangrove ecosystems. *Biol. Lett.* **14**, 20180237 (2018).
14. Andersen, F. Ø. & Kristensen, E. Oxygen microgradients in the rhizosphere of the mangrove Avicennia marina. *Mar. Ecol. Prog. Ser.* **44**, 201–204 (1988).
15. Duarte, C. M. Seagrass depth limits. *Aquat. Bot.* **40**, 363–377 (1991).

16. Bowman, G. & Harvey, N. Geomorphic Evolution of a Holocene Beach-Ridge Complex, LeFevre Peninsula, South Australia. *J. Coast. Res.* **2**, 345–362 (1986).
17. Duarte, C. M., Middelburg, J. J. & Caraco, N. Major role of marine vegetation on the oceanic carbon cycle. *Biogeosciences* **2**, 1–8 (2005).
18. Fahner, N. A., Shokralla, S., Baird, D. J. & Hajibabaei, M. Large-Scale Monitoring of Plants through Environmental DNA Metabarcoding of Soil: Recovery, Resolution, and Annotation of Four DNA Markers. *PLOS ONE* **11**, e0157505 (2016).
19. Foster, N. R. *et al.* A Multi-Gene Region Targeted Capture Approach to Detect Plant DNA in Environmental Samples: A Case Study From Coastal Environments. *Front Ecol. and Evol.* **9**, (2021).
20. Deiner, K. *et al.* Environmental DNA metabarcoding: Transforming how we survey animal and plant communities. *Mol. Ecol.* **26**, 5872–5895 (2017).
21. Murchie, T. J. *et al.* Collapse of the mammoth-steppe in central Yukon as revealed by ancient environmental DNA. *Nat Commun* **12**, 7120 (2021).
22. Lentz, D. L. *et al.* Environmental DNA reveals arboreal cityscapes at the Ancient Maya Center of Tikal. *Sci Rep* **11**, 12725 (2021).
23. Woodward, C. A. & Gadd, P. S. The potential power and pitfalls of using the X-ray fluorescence molybdenum incoherent: Coherent scattering ratio as a proxy for sediment organic content. *Quat. Int.* **514**, 30–43 (2019).
24. McCloskey, T. A., Smith, C. G., Liu, K., Marot, M. & Haller, C. How Could a Freshwater Swamp Produce a Chemical Signature Characteristic of a Saltmarsh? *ACS Earth Space Chem.* **2**, 9–20 (2018).
25. Rothwell, R. G. & Croudace, I. w. Twenty Years of XRF Core Scanning Marine Sediments: What Do Geochemical Proxies Tell Us? in *Micro-XRF Studies of Sediment Cores: Applications of a non-destructive tool for the environmental sciences* (eds. Croudace, I. W. & Rothwell, R. G.) 25–102 (Springer Netherlands, 2015). doi:10.1007/978-94-017-9849-5_2.
26. Becker, L. W. M. *et al.* Palaeo-productivity record from Norwegian Sea enables North Atlantic Oscillation (NAO) reconstruction for the last 8000 years. *npj Clim Atmos Sci* **3**, 1–12 (2020).
27. Saintilan, N., Rogers, K., Mazumder, D. & Woodroffe, C. Allochthonous and autochthonous contributions to carbon accumulation and carbon store in southeastern Australian coastal wetlands. *Estuar. Coast. Shelf Sci.* **128**, 84–92 (2013).
28. Kaal, J., Martínez Cortizas, A., Mateo, M.-Á. & Serrano, O. Deciphering organic matter sources and ecological shifts in blue carbon ecosystems based on molecular fingerprinting. *Sci. Total Environ.* **742**, 140554 (2020).
29. Belperio, A. P., Hails, J. R., Gostin, V. A. & Polach, H. A. The stratigraphy of coastal carbonate banks and Holocene sea levels of northern Spencer Gulf, South Australia. *Mar. Geol.* **61**, 297–313 (1984).
30. Telfer, K. W. & Malone, G. A People's Living Cultural Landscape.
31. Telfer, S. Torrens Island biodiversity action plan. (2013).

32. Edyvane, K. Edyvane, K.S. (1999). Coastal and marine wetlands in Gulf St Vincent, South Australia: understanding their loss and degradation. *Wetl. Ecol. Manag.* **7**, 83–104 (1999).
33. Glew, J. R., Smol, J. P. & Last, W. M. Sediment Core Collection and Extrusion. in *Tracking Environmental Change Using Lake Sediments: Basin Analysis, Coring, and Chronological Techniques* (eds. Last, W. M. & Smol, J. P.) 73–105 (Springer Netherlands, 2001). doi:10.1007/0-306-47669-X_5.
34. Ficetola, G. F., Taberlet, P. & Coissac, E. How to limit false positives in environmental DNA and metabarcoding? *Mol. Ecol. Resour.* **16**, 604–607 (2016).
35. Hermans, S. M., Buckley, H. L. & Lear, G. Optimal extraction methods for the simultaneous analysis of DNA from diverse organisms and sample types. *Mol. Ecol. Resour.* **18**, 557–569 (2018).
36. Lemmon, A. R., Emme, S. A. & Lemmon, E. M. Anchored Hybrid Enrichment for Massively High-Throughput Phylogenomics. *Syst. Biol.* **61**, 727–744 (2012).
37. Corinaldesi, C., Beolchini, F. & Dell'anno, A. Damage and degradation rates of extracellular DNA in marine sediments: implications for the preservation of gene sequences. *Mol. Ecol.* **17**, 3939–3951 (2008).
38. Glenn, T. C. *et al.* Adapterama I: universal stubs and primers for 384 unique dual-indexed or 147,456 combinatorially-indexed Illumina libraries (iTru & iNext). *PeerJ* **7**, e7755 (2019).
39. Hollingsworth, P. M., Graham, S. W. & Little, D. P. Choosing and Using a Plant DNA Barcode. *PLOS ONE* **6**, e19254 (2011).
40. Li, W. & Godzik, A. Cd-hit: a fast program for clustering and comparing large sets of protein or nucleotide sequences. *Bioinformatics* **22**, 1658–1659 (2006).
41. Waycott, M., Van Dijk, K. & Biffin, E. *A hybrid capture RNA bait set for resolving genetic and evolutionary relationships in angiosperms from deep phylogeny to intraspecific lineage hybridization*. http://biorxiv.org/lookup/doi/10.1101/2021.09.06.456727 (2021) doi:10.1101/2021.09.06.456727.
42. Schubert, M., Lindgreen, S. & Orlando, L. AdapterRemoval v2: rapid adapter trimming, identification, and read merging. *BMC Res. Notes* **9**, 88 (2016).
43. Schubert, M. *et al.* Characterization of ancient and modern genomes by SNP detection and phylogenomic and metagenomic analysis using PALEOMIX. *Nat Protoc* **9**, 1056–1082 (2014).
44. Li, H. Aligning sequence reads, clone sequences and assembly contigs with BWA-MEM. Preprint at http://arxiv.org/abs/1303.3997 (2013).
45. Foster, N. R. *et al.* A targeted capture approach to generating reference sequence databases for chloroplast gene regions. *Ecol. Evol.* **12**, e8816 (2022).
46. NCBI Resource Coordinators. Database resources of the National Center for Biotechnology Information. *Nucleic Acids Res.* **46**, D8–D13 (2018).
47. Li, H. A statistical framework for SNP calling, mutation discovery, association mapping and population genetical parameter estimation from sequencing data. *Bioinformatics* **27**, 2987–2993 (2011).

48. R Core Team, R. R: A language and environment for statistical computing. 2018. (2018).
49. Chamberlain, S. A. & Szöcs, E. taxize: taxonomic search and retrieval in R. *F1000Research* **2**, (2013).
50. Drost, H.-G., Gabel, A., Liu, J., Quint, M. & Grosse, I. myTAI: evolutionary transcriptomics with R. *Bioinformatics* **34**, 1589–1590 (2018).
51. Wickham, H., François, R., Henry, L., Müller, K. & Wickham, M. H. A Grammar of Data Manipulation. *R package version 1.0.2.* **8**, (2019).
52. Gagolewski, M. stringi: Fast and Portable Character String Processing in R. *J. Stat. Softw.* **103**, 1–59 (2022).
53. Wickham, H. & Wickham, M. H. Simple, Consistent Wrappers for Common String Operations. *R package version 1.4.0* (2019).
54. Wickham, H. & Henry, L. tidyr: Tidy Messy Data. *R package version 1.0.0.* (2019).
55. McMurdie, P. J. & Holmes, S. phyloseq: An R Package for Reproducible Interactive Analysis and Graphics of Microbiome Census Data. *PLOS ONE* **8**, e61217 (2013).
56. Wood, S. & Wood, M. S. Package 'mgcv'. *R package version* **1**, 729 (2015).
57. Ramsey, C. B. Deposition models for chronological records. *Quat. Sci. Rev.* **27**, 42–60 (2008).
58. Hogg, A. G. *et al.* SHCal20 Southern Hemisphere Calibration, 0–55,000 Years cal BP. *Radiocarbon* **62**, 759–778 (2020).
59. Heaton, T. J. *et al.* Marine20—The Marine Radiocarbon Age Calibration Curve (0–55,000 cal BP). *Radiocarbon* **62**, 779–820 (2020).
60. Ulm, S. *et al.* Australian marine radiocarbon reservoir effects: ΔR atlas and ΔR calculator for Australian mainland coasts and near-shore islands. *Radiocarbon* (2023).
61. Evans, G., Augustinus, P., Gadd, P., Zawadzki, A. & Ditchfield, A. A multi-proxy μ-XRF inferred lake sediment record of environmental change spanning the last ca. 2230 years from Lake Kanono, Northland, New Zealand. *Quat. Sci. Rev.* **225**, 106000 (2019).
62. Jolliffe, I. T. *Principal component analysis for special types of data*. (Springer, 2002).
63. Killick, R. & Eckley, I. A. changepoint : An *R* Package for Changepoint Analysis. *J. Stat. Soft.* **58**, (2014).
64. Wickham, H. An introduction to ggplot: An implementation of the grammar of graphics in R.

Figures

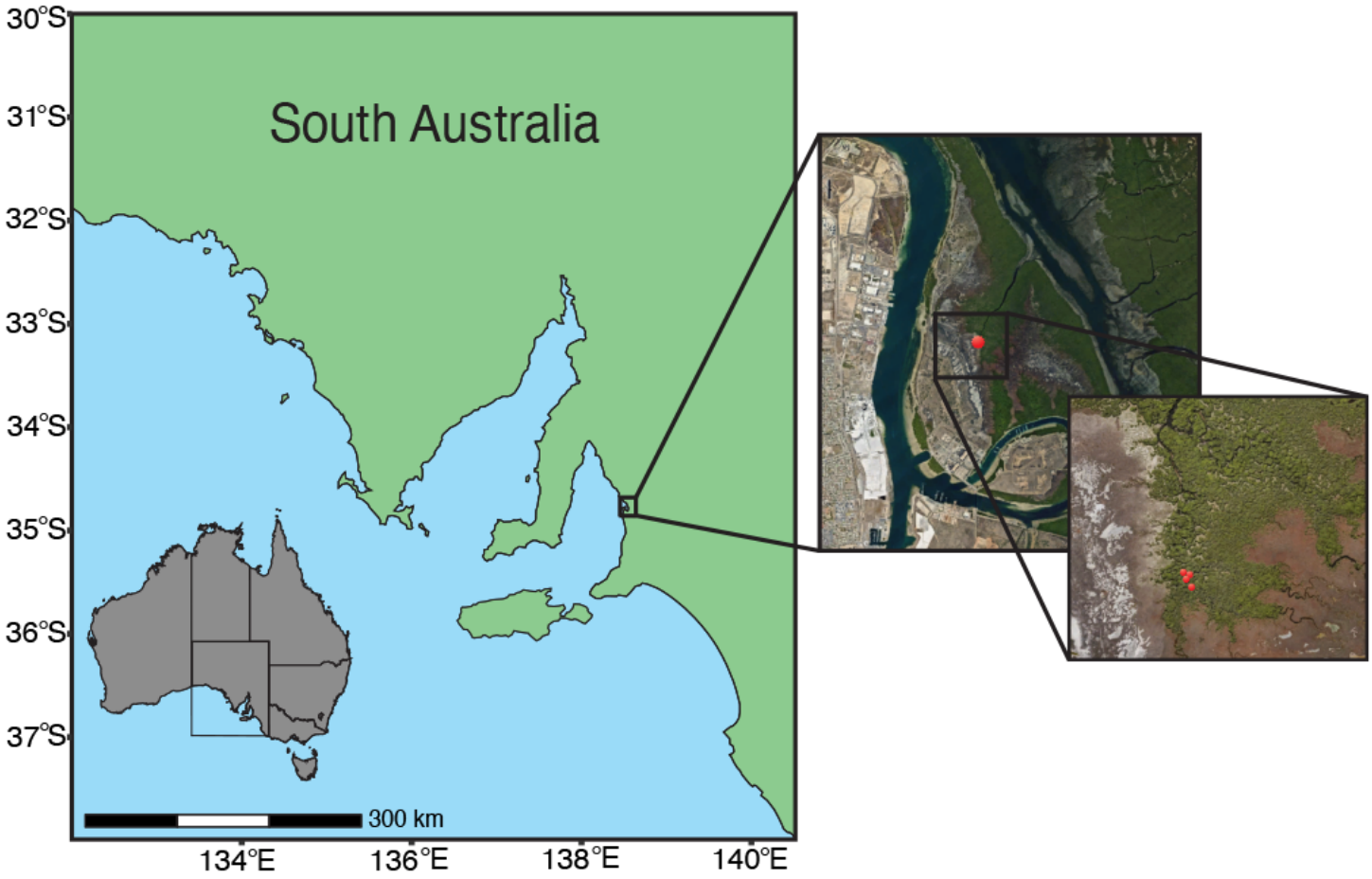

Figure 1

Four soil cores were collected for this study from Torrens Island, South Australia, Australia. The red dots indicate where the four cores were collected in 2017 (Core 1) and 2018 (Cores 2 - 4).

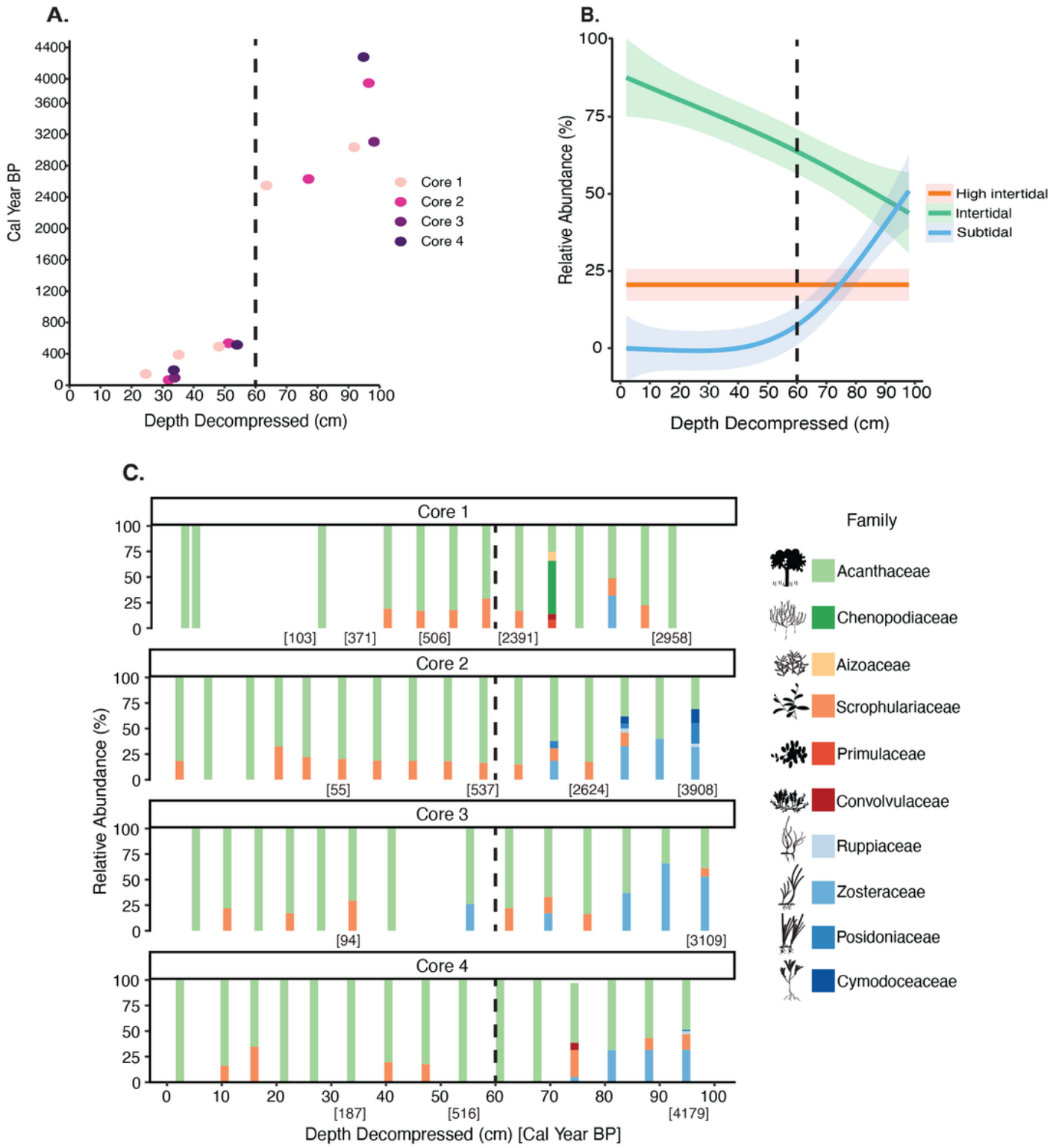

Figure 2

A. ^{14}C dating results. **B**. Changes in high intertidal, intertidal and subtidal vegetation types plotted against decompressed depth using a gam smoothing term. **C.** Breakdown of plant community composition by relative abundance with decompressed depth, colours indicate vegetation type; Red/orange = high intertidal, green = intertidal and blue = subtidal. Silhouettes (Integration and Application Network, ian.umces.edu/media-library) represent the species detected within each family; Acanthaceae =

Avicennia marina, Aizoaceae = *Disphyma crassifolium,* Chenopodiaceae = *Salicornia* and *Tecticornia* (genus level resolution only), Convolvulaceae = *Wilsonia humilis*, Cymodoceaceae = *Amphibolis antarctica*, Posidoniaceae = *Posidonia australis*, Primulaceae = *Samolus repens*, Ruppiaceae = *Ruppia maritima*, Scrophulariaceae = *Myoporum insulare*, Zosteraceae = *Zostera nigricaulis*. ^{14}C dates are indicated in brackets. The dashed line on each figure is placed at the approximate significant changepoint identified by the changepoint analyses (see methods), separating Units 1 and 2.

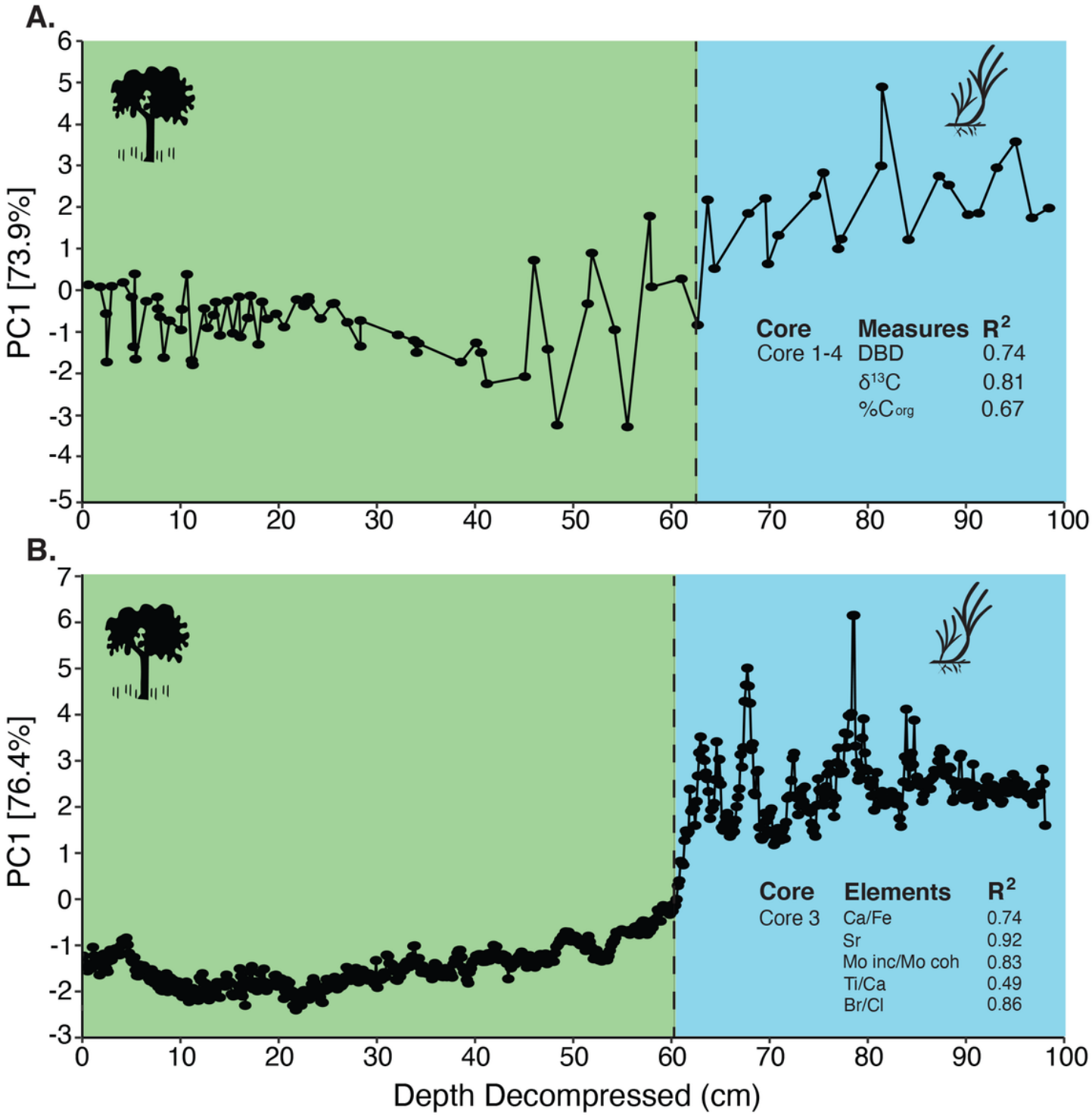

Figure 3

Principal Component Analysis (PCA) results for **A.** Dry bulk density, $\delta^{13}C$ and $\%C_{org}$ and **B.** Elements; Moly ratio, Ti/Ca, Br/Cl, Sr(normalised) and Ca/Fe for soil Cores 1-4 and Core 3, respectively. Principal component 1 explained 73.9% of the variance in A and 76.4% in B. How well each variable correlated to PC1 is shown by the R^2 values. The dashed line is placed at the significant change points identified by change point analysis (see methods). Colours indicate Units and dominant vegetation type; green/intertidal = Unit 1, blue/subtidal = Unit 2. Silhouettes depict the dominant vegetation found in each unit with *Avicennia marina* in Unit 1 and *Zostera nigricaulis* in Unit 2 (Integration and Application Network, ian.umces.edu/media-library).

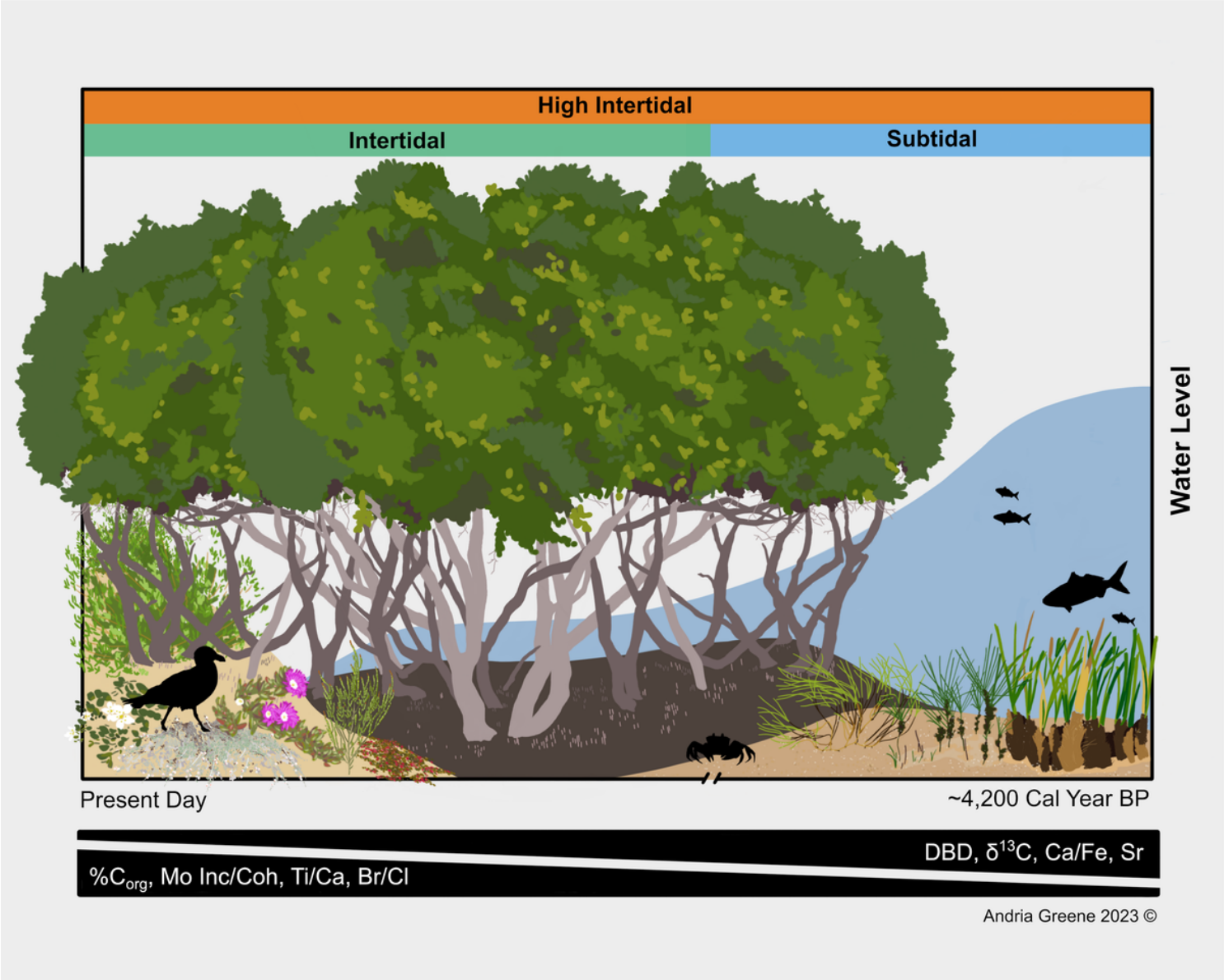

Figure 4

Conceptual diagram of historical coastal vegetation change uncovered at Torrens Island (South Australia). ^{14}C dates are shown on the x-axis with water level on the y-axis. Wedges on the bottom of the

figure indicate which measured variables increased and decreased over time. Plant community type is indicated by coloured bars at the top of the image.

Supplementary Files

This is a list of supplementary files associated with this preprint. Click to download.

- SupplementaryMaterial.docx